Applied Thermal Engineering 253 (2024) 123779

Contents lists available at ScienceDirect

Applied Thermal Engineering

journal homepage: www.elsevier.com/locate/apthermeng

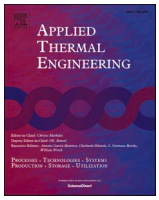

Research Paper

Rheological aspects of solid-to-liquid phase transitions in paraffin wax/bitumen blends for thermal energy storage applications

C. Gutiérrez-Blandón, A.A. Cuadri, P. Partal, A. Tenorio-Alfonso, C. Delgado-Sánchez, F.J. Navarro *

Pro²TecS-Chemical Process and Product Technology Research Centre, Department of Chemical Engineering, ETSI, Campus de "El Carmen", Universidad de Huelva, 21071 Huelva, Spain

ARTICLE INFO

Keywords:
Bitumen
Paraffin wax
Phase change material
Rheology
DSC
Thermal storage

ABSTRACT

This paper correlates the evolution of the rheological and thermal properties with microstructure during the phase change of a blend of bitumen with a selected paraffin wax, having a melting point centred around 60 °C, for the development of bituminous based membranes for thermal energy storage applications. For this purpose, temperature sweep tests within the linear viscoelastic range, stationary state flow curves, Differential Scanning Calorimetry (DSC), polarised optical microscopy observations and solar irradiation tests were performed. The reported rheological results clearly point out a gel-like behaviour for both paraffin and paraffin/bitumen blend that is preserved almost up to the end of the phase change interval. This is consequence of the development of a network of interconnected crystals of paraffin wax which progressively disappear as temperature increases. Interestingly, a weak gel structure is kept even at low crystallinity levels since only a few junctions among structures are necessary to build a spanning network. Finally, the large degree of crystallinity of paraffin wax retained in the bitumen/paraffin wax is behind its thermoregulation ability, as was corroborated by solar irradiation tests. Therefore, results indicated the great potential of these formulations for thermal energy storage and related applications.

1. Introduction

Currently, the global growth in energy demands has encouraged the scientific community to focus on the development of new technologies and the search for new materials for solar capture and thermal energy storage. In this sense, bitumen-based products may become a promising alternative, as their black colour leads to a low albedo or solar reflection and therefore results in a large solar absorption capacity [1].

Bitumen is the heaviest fraction of the crude oil obtained from the bottom of vacuum distillation towers, composed of a combination of relatively high molecular weight molecules, usually classified in terms of polarity into families of compounds: Saturates, Aromatic, Resins and Asphaltenes, known as SARAs fractions [2].

Apart from the traditional use of bitumen as a binder of mineral aggregates in road pavements, its waterproofing nature and compatibility with polymeric additives make it extensively used in the formulation of roofing and waterproofing membranes [3,4]. More recently, new applications have arisen related to energy storage and/or thermoregulation technologies. For example, several authors have analysed the potential use of bituminous materials as solar collectors in road pavements (solar pavements), able to harvest and store thermal energy from sun radiation [5,6]. In addition, some modified bituminous based membranes may provide significant thermoregulation effect particularly useful to mitigate heat island effects in cities and to reduce maximum ambient temperatures [5,7–9].

In general, bitumen modification for energy storage and thermoregulation is based on the incorporation of the so-called phase change materials (PCMs), capable of absorbing and releasing latent heat during the phase change process, typically between solid and liquid states. Even though a large number of PCMs have been proposed in the literature, paraffin waxes are the most preferred energy storage material within range of 0 to 75 °C because of their low cost, low vapour pressure, chemical stability and safety, high latent heat, low super-cooling, thermal stability for thermal cycles, tuneable phase change temperature, etc. [10,11].

Recently, there has been growing interest in analysing the feasibility of modifying road paving bitumen with PCM for road paving

* Corresponding author at: Pro2TecS-Chemical Process and Product Technology Research Centre, Department of Chemical Engineering, ETSI, Campus de "El Carmen", Universidad de Huelva, 21071 Huelva, Spain.
E-mail address: frando@uhu.es (F.J. Navarro).

https://doi.org/10.1016/j.applthermaleng.2024.123779
Received 4 March 2024; Received in revised form 30 May 2024; Accepted 20 June 2024
Available online 22 June 2024

Nomenclature

Nomenclature with dimensions and abbreviations.

BP	Bitumen paraffin blend
DSC	Differential Scanning Calorimetry
Heat Flow	from DSC experiments (W/g)
G'	Storage Modulus (Pa)
G''	Loss Modulus (Pa)
G*	Complex Shear Modulus (Pa): $\|G^*\| = \sqrt{G'^2 + G''^2}$
ω	Angular Frequency (rad/s)
δ	Phase angle (°)
η	Viscosity (Pa·s)
η_0	Zero-shear limiting viscosity (Pa·s)
$\dot{\gamma}$	Shear rate (1/s)

applications, primarily with the goal of achieving temperature regulation effects and improving thermo-mechanical properties, aging resistance, fatigue resistance, etc. [8]. A number of PCMs have proven to be suitable for these purposes such as paraffin waxes [11,12], fatty acids (Lauric and Stearic acid) [13], fatty alcohols and sugar alcohols (Tetradecyl alcohol, Neopentylene glycol, D-Manitol, etc.) [13,14], Polyethylene glycols (from 1000 to 4000 g/mol) [13,15–17] and selected polyurethanes with solid–solid phase transitions [7].

Regarding roofing and waterproofing systems, there is limited bibliography available on the integration of PCM into bituminous membranes. Thus, a few studies have pointed out that the use of PCMs in traditional roofing membranes contribute to reducing energy consumption in houses due to the lower heating energy demand [18,19].

In general, the most widely used technology to add PCM to bitumen is through encapsulation or stabilization methods, which significantly increases its fabrication cost and reduces the thermal conductivity of the final product, making the heat storage and release processes less efficient [8,10]. In the case of bituminous membranes for building applications, as a consequence of the relatively large amount of PCM to be used, they are usually enclosed by means of a multilayer envelope [19].

Consequently, even though direct incorporation of PCM to bitumen is preferred from a cost point of view, this method needs specific analysis about miscibility or compatibility among components, especially during the phase change process, in order to maximize the energy storage capacity and achieve optical rheological properties. Therefore, a partial compatibility between PCM and bitumen is needed to develop a multiphase morphology with adequate thermomechanical properties while crystalline structures are preserved, which is an essential aspect to keep latent heat [3,12,20].

In addition, the phase change process, usually exhibits multiple transitions in a wide temperature interval, that strongly affects the performance properties and thermal behaviour. In the particular case of paraffin waxes, it is well established that they experience multi-step phase transitions that may overlap and mutually affect each other, during heating experiments. Then, depending on factors such as molecular structure, molecular weight, impurities, etc., several premelting solid–solid phase transitions are typically observed before the solid-to-liquid phase transition [21,22].

In this study, a selected paraffin wax having a melting peak of approximately 60 °C, was blended with bitumen, to analyse the rheological properties, microstructure and thermal behaviour during heating experiments. In particular, the evolution of crystalline structures within the phase change temperature interval from 50 to 70 °C, has been correlated with the resulting rheological behaviour and developed microstructure. To that end, neat compounds and the bitumen/paraffin blend were subjected to linear viscoelastic measurements, stationary flow tests, differential scanning calorimetry and cross-polarized optical microscopy to determine the phase transitions and morphology. Finally, the thermoregulation ability of the paraffin/bitumen blend was assessed by means of cooling tests following heating induced by simulated solar irradiation.

2. Experimental

2.1. Materials

A commercial-grade paraffin with a melting temperature around 60 °C was used in this study, as PCM, supplied by Panreac-AppliChem (Spain). An asphaltic 100/150 penetration grade bitumen donated by REPSOL, was employed to formulate the blends (Table 1), having a ring and ball softening point of 41.0 °C and a penetration of 105 dmm. Its chemical composition according to SARAs fractionation is: Saturates 7.4 wt%, Aromatics 57.6 wt%, Resins 15.1 wt% and Asphaltenes 19.9 wt%.

2.2. Sample preparation

Bitumen/paraffin wax blend was obtained using a high-shear processing device (rotor–stator homogenizer Silverson L5M-A) following the protocol outlined below. Approximately 250 g of the blend, containing 40 wt% of paraffin wax, was preconditioned at a mixing temperature of 150 °C in aluminium cans, and then mixed at a rotation rate of 3500 rpm for 15 min. After processing, samples were poured into silicon moulds of the appropriate dimensions for rheological or DSC measurements and allowed to cool down to room temperature.

2.3. Tests and measurements

2.3.1. Rheological and technological characterisation

Oscillatory frequency sweep tests, were carried from 0.01 to 100 rad/s, at selected constant temperatures (50, 55, 60 and 70 °C) within the phase change interval. Additionally, oscillatory temperature ramp tests, at a heating rate of 1 °C/min, were accomplished at a constant frequency of 10 rad/s, over the same temperature range. These oscillatory shear measurements were carried out at strains within the linear viscoelastic region, previously determined at every temperature. Viscous flow tests, from 10^{-6} to 10^{2} s^{-1}, were performed in the control stress mode at the temperatures of 50, 55, 60, 61, 62 and 70 °C. All rheological tests were conducted is a controlled-stress Physica MCR-301 rheometer (Anton Paar, Austria) using a plate-plate geometry (25 mm diameters with 1–2 mm gap).

2.3.2. Optical microscopy

Microstructural changes of paraffin and bitumen/paraffin wax blend (BP) with increasing temperature were analysed by optical microscopy using simultaneously crossed polarised and non-polarised light, in an Olympus BX51 (Japan) microscope coupled to an LTS-350 Heating-Freezing Stage controlled by a Linkam TP94 (Linkam Scientific Instruments, UK). In order to ensure the same thermal history, a drop of hot sample (melted paraffin or blend) was placed on a flat slide, previously conditioned at 100 °C, and covered by a cover glass and let to cool down to 25 °C at a controlled rate of 1 °C/min. Then, glass slides were progressively heated up to the target temperature (from 40 to 70 °C) and tempered for 10 min for optical observation.

Table 1
Detailed properties of the base bitumen.

Technological properties	
Penetration (dmm)	105
Softening point (°C)	41.0
Chemical composition	
Saturates (wt.%)	7.4
Aromatics (wt.%)	57.6
Resins (wt.%)	15.1
Asphaltenes (wt.%)	19.9

2.3.3. DSC tests

Differential Scanning Calorimetry (DSC) measurements were conducted on all samples using a Q-250 DSC calorimeter (TA Instruments, USA). Each sample (10–20 mg) was sealed in conventional hermetic aluminium pans, and scanned in a flowing nitrogen atmosphere (50 mL·min^{-1}) according to the following procedure, at heating /cooling rates of 10 °C/min: (i) isothermal at 70 °C for 10 min, (ii) cooling scan to 20 °C, (iii) isothermal at 20 °C for 10 min, (iv) heating scan to 70 °C.

2.3.4. Solar irradiation and cooling tests

Samples of bitumen and bitumen/paraffin wax blend (BP) were heated up to constant temperature by irradiating simulated solar light with a Xenon lamp HXF300-T3 (Beijing China Education Au-light Technology Co., Ltd, China), using a filter AM 1.5G (300–1100 nm).

Cylindrical Samples (42 mm diameter and 8.5 mm thickness) were heated by an average irradiation of 1385 ± 32 W/m^2 over the entire binder surface (measured by a pyranometer SMP3, Kipp & Zonnen, Netherlands) until the surface reached a constant temperature, and then let to cool down. A thermocouple was placed at 2.2 mm away from the exposed surface to determine the temperature evolution with time. The wall of the specimen was insulted with a 77.6 mm-thickness isolator (k = 0.044 W/m °C, thermal conductivity), whereas its bottom side was in contact with isothermal heat sink, with selected cooling or sink temperatures of T_s = 46.5 °C.

3. Results and discussion

3.1. Thermo-rheological properties evolution in temperature ramp tests

The here used paraffin is a macrocrystalline wax, chemically composed of mixtures n-paraffins and, in minor extent, *iso*-paraffins having minimal branching [23], obtained through the separation of heavy distillate fractions in the refining process.

DSC thermogram for paraffin wax, portrayed in Fig. 1A, reveals its highly crystalline nature, exhibiting a wide and asymmetric phase change peak during heating, originally attributed to the melting of crystalline structures [24]. In general, the observed broad peak is associated to the presence of paraffin chains of different lengths with close molecular weights, which gradually undergo phase transitions to the isotropic liquid state [25]. By comparing the melting interval reported in Fig. 1A with those of pure n-alkanes reported in the bibliography, it can be estimated that the paraffin wax is mainly composed of alkanes in the range C25-C28 [26]. The presence of a shoulder in the heating scan, that leads to a pronounced left asymmetry of the peak, could be indicative of another first order transition. In fact, it has been widely reported that pure alkanes, their mixtures and industrial paraffins usually exhibit solid-to-solid transitions prior to their melting [27]. In order to shed some light on this issue, in this paper DSC and rheological tests have been compared. In this sense, in Fig. 1 attempts to correlate the calorimetric transitions with the complex shear modulus (G*) decay as temperature increases. According to Fig. 1B, paraffin wax clearly shows a two-step decay process of G*, characterized by an initial decrease stage, reaching a flattening of the slope up to approximately 53 °C, followed by a sharper drop of G* by several orders of magnitude into the flow region. By comparing the temperature interval where the first softening occurs with DSC data, as the threshold rheological temperature matches the inflection point of the heat flow, it seems that this is mainly driven by solid-to-solid transitions of the paraffin. This result is in agreement with literature data of paraffins since a similar intermediate mesophase region to that shown here, between the glassy state and the isotropic liquid phase, is frequently reported [23,28,29]. At a molecular scale, this is a consequence of the transition of the paraffin chains into a premelting mesophase, where several rotator phases may appear. Thus, it is well established since normal paraffins, alcohols, and other hydrocarbons molecules may pass consecutively through one or several rotator phases, which are intermediate stages between the fully ordered

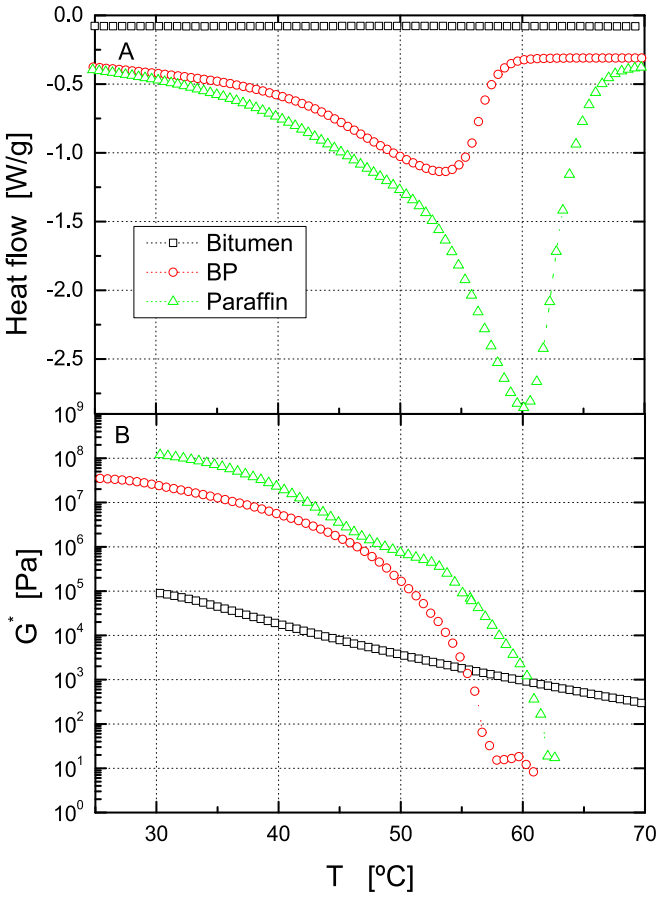

Fig. 1. Evolution with temperature of heat flow from DSC (A) and complex shear modulus from temperature sweep tests (B) of paraffin wax, bitumen and the blend.

crystalline phase and the disordered isotropic liquid, formed by layered three-dimensional structures that only present a rotational degree of freedom around the molecular axes [24,25,28].

Considering the industrial nature of the sample and the difficulty in isolating rotator phases from temperature sweep tests, even for pure n-alkanes, the observed mesophase region is developed by the existence of several transitions between rotator phases [30]. In contrast to the crystalline state, in rotator phases, the molecular chains can rotate quasi-freely about their axes, leading to less organized structures and a softer mechanical response [29].

In contrast, as indicated in Fig. 1, neat bitumen only shows a steady fall of G* with temperature with no relevant thermal events within this temperature interval, which is indicative of its direct transition from the glassy to the Newtonian region. As expected, the binary blend BP presents an intermediate rheological behaviour from that shown by their parent pure compounds. However, its thermomechanical response is closer to that of the paraffin wax and, therefore, associated to the solid-to-liquid transitions of the paraffin phase, given the reported DSC profile (Fig. 1B). In this case, even though the mesophase region is no longer observed in the blend, the inflection point in the melting DSC scan at around 46 °C would be indicative of the mentioned transitions between rotator phases as it aligns with the temperature at which the slope changes in the temperature sweep test.

It is worth mentioning that, normalised phase change enthalpies per gram of paraffin in the mixture, calculated from DSC curves, are only slightly reduced in 3.5 % (from 209.1 to 201.9 J/(g of paraffin) for pristine paraffin and the blend, respectively), and the peak temperature of the melting endotherm lowers from 60.2 to 53.5 °C. This result points out a minor partial compatibility between bitumen compounds and the

crystals of paraffin [4,12]. Interestingly, despite this, the degree of crystallinity of paraffin phase in the blend is largely retained which is particularly useful for thermal energy storage applications.

Finally, it is important to note that, for both paraffin and BP, the drop of G* is very steep within the melting DSC interval. Nevertheless, due to the low sensitivity of this test close to the isotropic stage it remains unclear whether the samples reach the terminal region of the mechanical spectrum.

3.2. *Evolution of linear viscoelastic properties under isothermal conditions*

As shown, isochronal dynamic temperature sweep tests, at constant deformation, provide general knowledge about phase transitions and rheological properties evolution with temperature during heating. However, in order to obtain detailed structural information under isothermal conditions, frequency sweep tests have been performed at selected temperatures within the phase change interval (Fig. 2A-2D).

Neat bitumen displays the expected progressive transition to the viscous flow region, with both moduli decreasing as the temperature rises, $\acute{G}>\acute{G}$, and low-frequency slopes reaching 2 for the elastic modulus and 1 for the loss modulus (Fig. 2) [31]. Conversely, paraffin and BP present a very different rheological response. In the case of paraffin wax, from 50 to 60 °C (Fig. 2A-C), G' and $\acute{G}$ intersect and gradually increase with frequency, with moduli consistently remaining 3 decades below the expected values of the glassy region, where the glassy modulus reaches approximately 10^9 Pa. As temperature increases in this interval, the crossover frequency is shifted to lower values and both moduli undergo a decrease of around one order of magnitude, yet still exhibit a similar qualitative behaviour [32,36]. Notably, at 60 °C, corresponding to the DSC melting peak temperature of pristine paraffin (Fig. 1A), high viscoelastic moduli persist, highlighting a significant influence of the remaining crystalline paraffin domains in the microstructure.

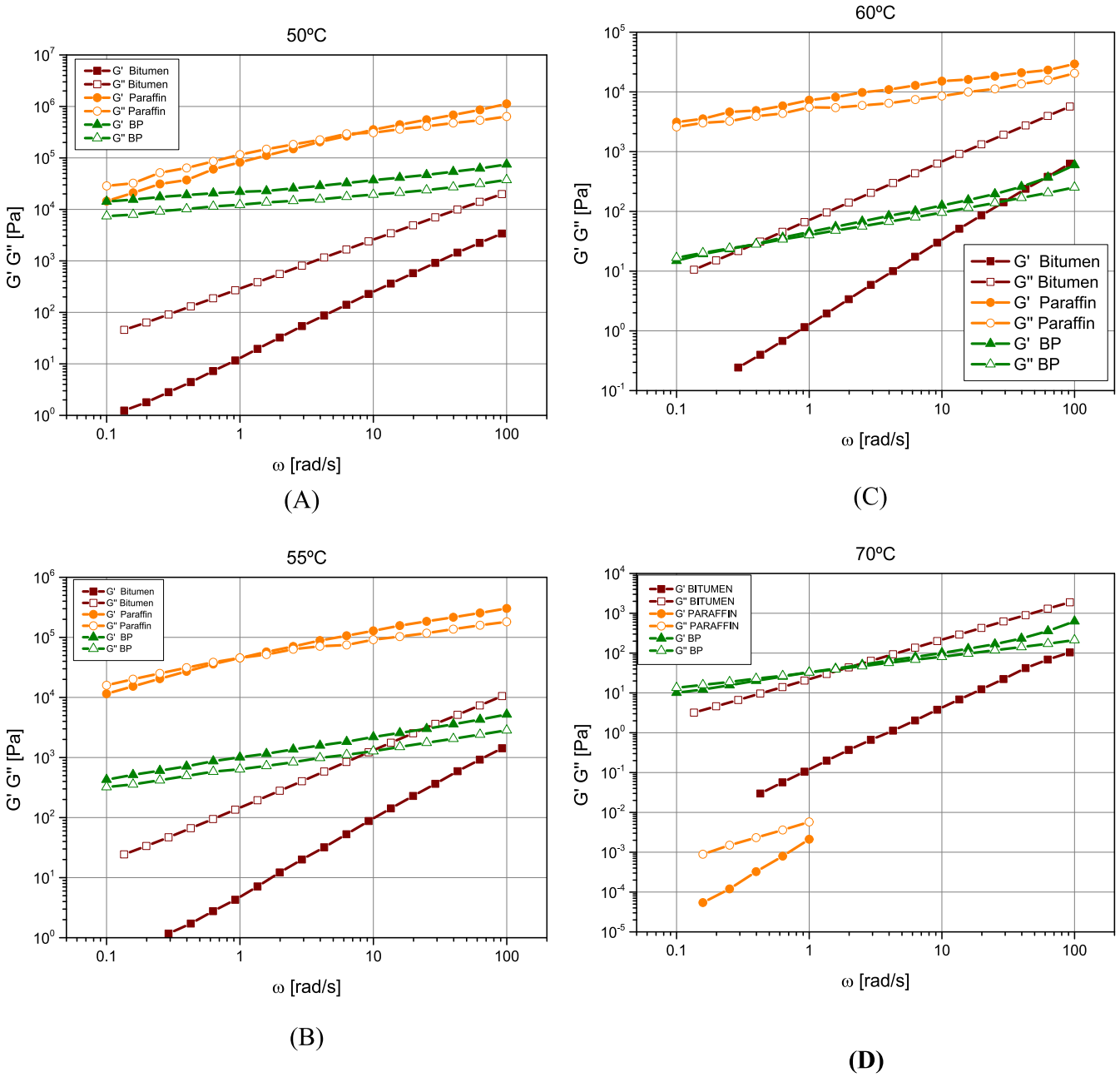

Fig. 2. Frequency dependence of the linear viscoelasticity functions $\acute{G}$ and $\acute{G}$ for paraffin wax, bitumen and their blend at (A) 50 °C, (B) 55 °C, (C) 60 °C and (D) 70 °C.

By contrast, at 70 °C a significant drop of elastic (Ǵ) and loss moduli (Ǵ) is noticed, reaching the flow region of the mechanical spectrum, corresponding to the isotropic liquid or melt region of paraffins [23]. When compared to isothermal neat bitumen curves, as expected, paraffin wax presents higher moduli values and lower slopes at 50 and 55 °C, an intermediate behaviour at 60 °C and significantly lower values after the complete melting of paraffin (70 °C).

The linear viscoelastic behaviour of the bitumen/paraffin blend is more complex with a distinct influence of both phases, depending on the testing temperature. Thus, at 50 and 55 °C, the elastic character predominates (Ǵ>Ǵ) with both moduli appearing parallel or nearly parallel throughout the frequency spectrum, displaying a typical behaviour of a critical gel [33]. Since 55 °C is approximately the DSC peak melting temperature, this result is indicative of the development of a continuous paraffin-rich phase within the blend, where the melting of paraffin wax leads to the reported softening with temperature. Then, as temperature increases, both moduli are progressively reduced, the slope of the curves increases and a crossover occurs. Surprisingly, at 70 °C, which exceeds the melting range observed in the DSC analysis of BP (Fig. 1), despite the individual components exhibit a terminal behaviour, the rheological response of the blend differs significantly, with slopes close to 0.5 and larger values than expected, particularly at low frequencies. This outcome hints a phase-separated morphology that persists beyond the melting of the paraffin, contributing to the reported high viscoelastic moduli.

Black diagrams curves (phase angle vs complex shear modulus) are very beneficial for characterising bituminous based materials, as they depict the evolution of time-independent functions that are highly sensitive to morphology changes. In this regard, Fig. 3 illustrates that while bitumen functions merge into a single common curve and the phase angle approaches 90° (Newtonian viscous region) as G* lowers, paraffin and BP display a markedly thermoreologically complex behaviour, associated with the first-order phase transitions of paraffin wax [34]. Paraffin wax curves points out the softening of the sample, as temperature increases near the melting point, i.e. a decrease in G* values until the DSC peak temperature is reached (60 °C) and an abrupt change to the flow region at 70 °C.

Interestingly, as the stiffening diminishes with increasing temperature, the elastic character is strengthened to the point where it becomes predominant ($\delta < 45°$) at the peak melting temperature (60 °C). From a structural perspective, this result is quite revealing since, according to DSC curve, despite only a minor fraction of paraffin molecules remain in the premelting mesophasic state (rotator phases) their contribution to the bulk properties is very significant.

In connection with the aforementioned points, given the presumption that BP is characterized by a continuous and dominant paraffin-rich phase, a similar rheological evolution is expected. Then, at 50 and 55 °C, temperatures very close to the DSC melting peak, a predominant elastic behaviour is clearly pointed out. However, at 60 and 70 °C, immediately after melting, the reported high complex shear modulus and low δ values, indicate the development of an ordered microstructure quite distinct from the liquid state post-melting.

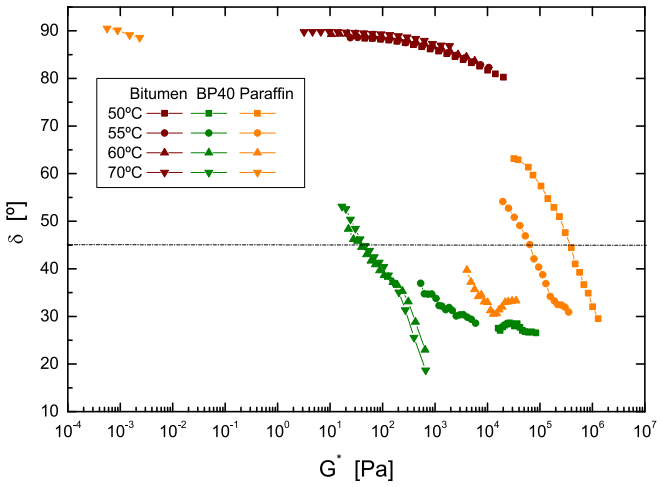

Fig. 3. Black diagram of paraffin wax, bitumen and the blend.

3.3. Evolution of the isothermal flow behaviour with temperature

Steady shear viscosity measurements provide valuable information about the structural development during the phase change temperature interval (Fig. 4). As shown in Fig. 4A, at 50–55 °C, paraffin wax presents the expected rheological behaviour of well-structured systems, showing a wide Newtonian plateau, at low shear rates, followed by a shear-thinning region. However, at 60–61 °C, the flow pattern changes as the Newtonian plateau is followed by a weak shear thickening (viscosity overshoot) before transitioning to the shear-thinning region. This unusual behaviour is only observed in a narrow temperature interval before to the melting endotherm since, at 62 or 70 °C, all paraffin molecules are fully melted exhibiting a low viscosity Newtonian behaviour. The occurrence of shear thickening prior to shear thinning has been found in solutions of amphiphilic or associating polymers, as well as in concentrated or reticulated SBS modified bitumen, where the common feature is the presence of dispersed structures (suspended molecules/micelles/particles) showing an associative behaviour [3]. This relatively unusual behaviour is frequently associated to non-permanent physical networks where, at a sufficiently strain rate, interactions among structures give rise to the formation of complex arrangements (networks or clusters), which restrict overall mobility and result in the viscosity overshoot [35]. As the bridges among structures rely on weak physical bonds, when the shear rate is further increased, the transient network is disrupted leading to subsequent shear thinning. In the case of paraffin wax, at temperatures close to the DSC melting peak, similar structures are expected to develop. Then, as the melting of molecules happens at different temperatures according their molecular weight, it appears that clusters of paraffin molecules in the premelting state (in the crystalline or rotator phase) are dispersed in a melted phase and possess the ability to physically interact among them, leading to the reported flow response under shear.

On the other hand, Fig. 4B displays the well-known response of unmodified bitumen, characterised by a wide Newtonian region followed by a shear-thinning zone. As temperature increases, bitumen becomes progressively less structured, resulting in lowered viscosity and increased threshold shear rate between both regimes [36].

Again, BP discloses a more complex rheological character and a much higher susceptibility to shear and temperature during melting (Fig. 4C). Thus, an apparent Newtonian region is noticed at low shear rates, followed by an extensive shear-thinning region at intermediate values and, finally, a second Newtonian region at high shear rates. As temperature increases within the phase change interval, the Newtonian viscosity is markedly reduced while the shear thinning behaviour becomes more pronounced, reaching differences of four orders of magnitude between the zero and infinite shear limiting viscosities. It is important to note that, even at the highest temperatures, the same qualitative flow behaviour remains apparent. This result confirms the development of a two-phase morphology that is preserved after paraffin phase melting.

3.4. Microstructural considerations

The presence and arrangement of paraffin wax structures during melting can be examined by optical microscopy, at constant temperatures, under cross-polarized light, since crystals appear as bright regions due to their anisotropy, whereas amorphous zones are shown as dark areas.

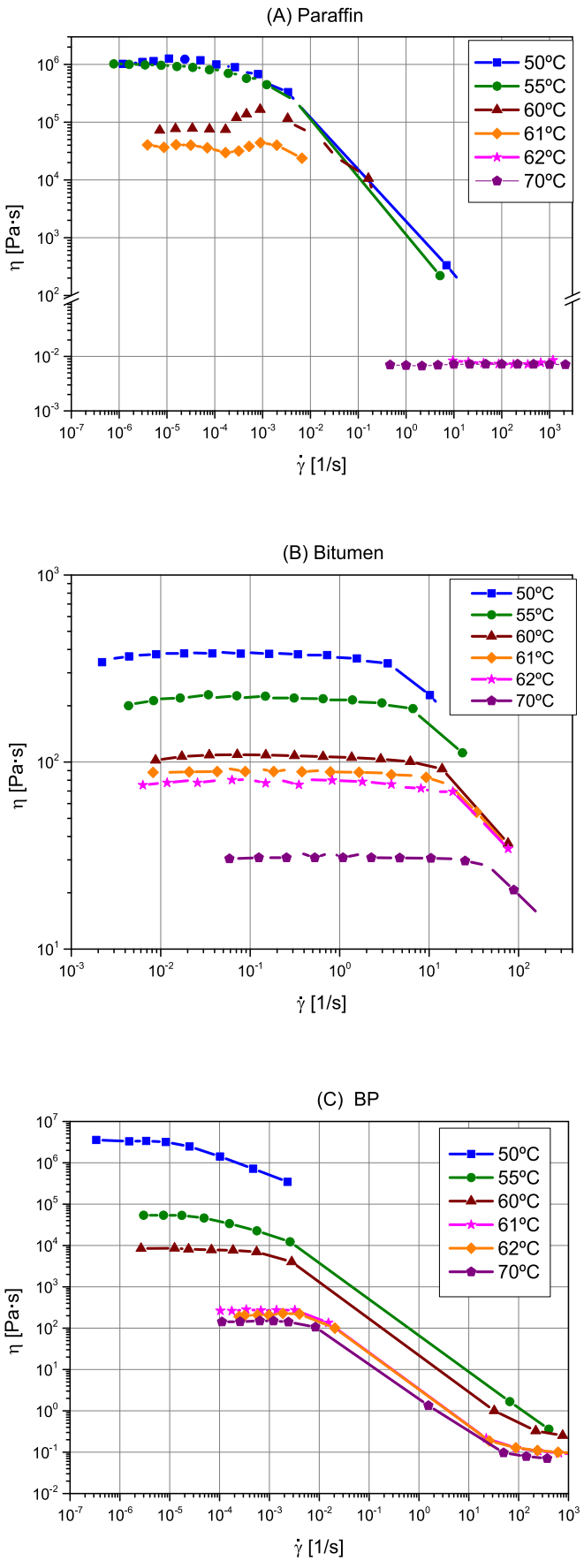

Fig. 4. Stationary flow curves at constant temperatures (from 50 to 70 °C) for (A) paraffin wax, (B) bitumen and (C) their blend.

As portrayed in Fig. 5, at the onset of the phase change (40 °C), needle-shaped crystals are clearly found in neat paraffin, which assemble to form a continuous network structure with dispersed amorphous regions [4,23,27]. Expectedly, shorter and thinner crystals and a higher content of amorphous regions are found in the BP blend, but the network is still preserved. Thus, this space-filling network of interlocking paraffin wax crystals is responsible for the reported linear viscoelastic behaviour [37].

When temperature is increased to 50 °C, despite viscoelastic moduli are reduced (Figs. 1 and 2), the network of paraffin crystals remains nearly unchanged, pointing out that rotator phase solid-to-solid transitions predominantly happen within this interval. In contrast, for BP sample, the network is less dense since crystallinity is reduced according to the reported DSC data (Fig. 1). Similarly, as both samples approach to the melting peak temperature, the amount and size of crystals are reduced while network gradually disappears, a fact that explain the drop of viscoelastic moduli. It is important to underline that, at temperatures close to the end of the melting process (roughly 60 °C), where only a small fraction of crystals remain, both samples present unexpectedly high storage and loss moduli (Fig. 2) and a pattern of flow curves of structured systems i.e. a zero shear limiting viscosities followed by a shear thinning region (Fig. 4). Thus, Fig. 6 shows the evolution of the zero-shear liming viscosity with temperature for all samples, pointing out that, while bitumen presents a consistent decrease, paraffin and BP exhibit a sharp drop at values close to the peak DSC melting point. Therefore, despite the gradual disappearance of the crystalline network with increasing temperature, the evolution of rheological properties does not mirror this progression. In order to shed some light on this issue, the maximum relative DSC crystallinity has been calculated, at selected temperatures within the melting interval. This was achieved by integrating the DSC phase change peak areas (Fig. 1), normalizing them by the paraffin concentration, and considering the enthalpy of ideal 100 % crystalline paraffin wax (293 J/g) (see equation (1):

$$RelativeDSCcrystallilnity(T) = \frac{\int_{298K}^{T} f_c H(T)}{293J/g} \quad (1)$$

where f_c is the paraffin concentration factor (100/40 for BP and 1 for paraffin) and $H(T)$ is the DSC heat flow at the temperature T. Additionally, surface area fraction of crystalline regions taken from crossed polarizers micrographs (Fig. 5) were also calculated by using ImageJ software. Then, with the aim to evaluate the relationship of the rheological behaviour with the remaining crystallinity during heating, Fig. 7 compares the temperature evolution of crystallinity with the decay of η_0. In general, at a specific temperature, crystallinity values obtained from optical measurements are slightly higher than those from DSC. This discrepancy is likely due to the former was taken at isothermal conditions whereas the latter was obtained at a selected heating rate which significantly impacts the results [38]. According to this, despite the thermal gap between them, both crystallinities approximately follow a similar progressive sigmoidal evolution with temperature. In contrast, for both paraffin and BP, η_0 experiences a much shaper drop that happens at clearly higher temperatures, and, then, this drastic rheological change occurs when crystallinity is very low. Hence, apart from paraffin crystals, a distinct microstructure is formed that influences the observed rheological properties. Nonetheless, it has been widely reported for crystallizing polymers, that a physical gel-structure can emerge even with low degree of crystallinity, because only a few junctions among structures are needed to stablish a spanning network [39].

The structures that form the network are loosely connected, resulting in a soft critical gel that influences the flow behaviour depicted in Fig. 4. Upon completion of the melting process, paraffin wax reaches a Newtonian behaviour whereas BP retains a weak gel structure. Then, Fig. 8 shows an unpolarised optical micrograph of BP, at 70 °C, above the melting interval, showing a structured system wherein a bitumen-rich phase is evident, likely due to an enrichment of asphaltenes.

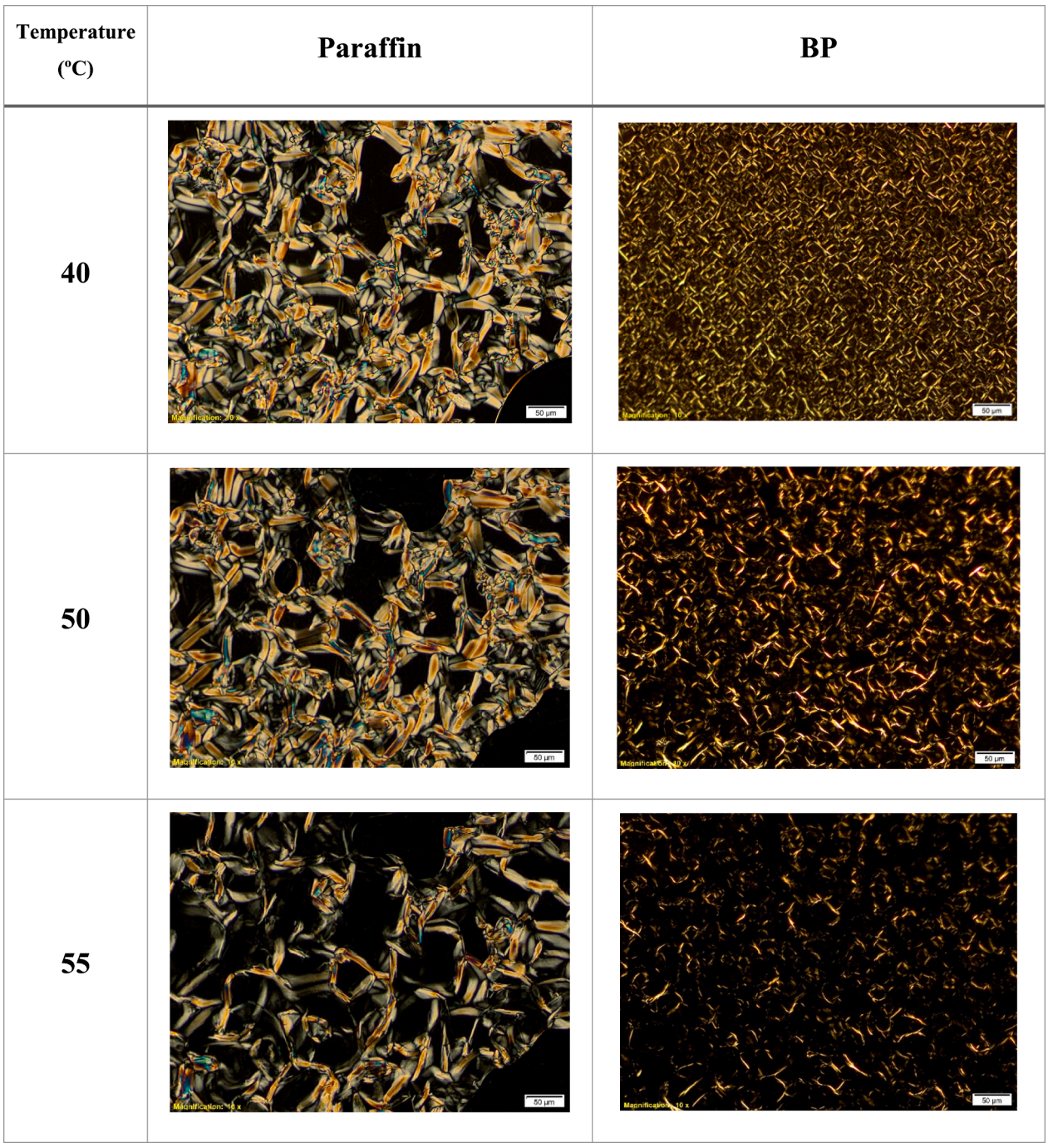

Fig. 5. Crossed-polarizers micrographs of paraffin wax and bitumen/paraffin blends, at selected temperatures within the phase change interval.

Therefore, this two-phase morphology would be responsible for the linear viscoelastic behaviour reported in Fig. 2D, given that the paraffin rich-phase is molten, a soft gel structure persists after the phase change leading the flow behaviour depicted in Fig. 4C.

3.5. Cooling behaviour after simulated solar irradiation

DSC and microscopy results revealed that the degree of crystallinity of paraffin phase in the BP blend is largely retained which can be of great interest for thermal energy storage applications. In this sense, the temperature regulation ability of BP blend was assessed following the experimental setup described in subsection 2.3.4. In this test, firstly, sample was heated by the action of a simulated solar irradiation (with an average irradiation of 1385 $\pm$ 32 W/m^2 over the entire binder surface) until the surface sample reaches a constant temperature. Afterwards, the solar lamp was turned off and the sample was let to cool until the final equilibrium temperature was attained. Fig. 9 shows the evolution with time of the temperature at 2.2 mm depth to sample surface, and its corresponding rate, for neat bitumen and BP sample during the cooling step. Interestingly, the thermoregulation ability of BP sample compared to its corresponding neat bitumen is clearly detected by higher temperatures and lower cooling rate. Thus, neat bitumen undergoes a rapid temperature drop, exhibiting its unique maximum cooling rate after ca. 135 s, until it reaches the equilibrium temperature after ca. 1000 s of

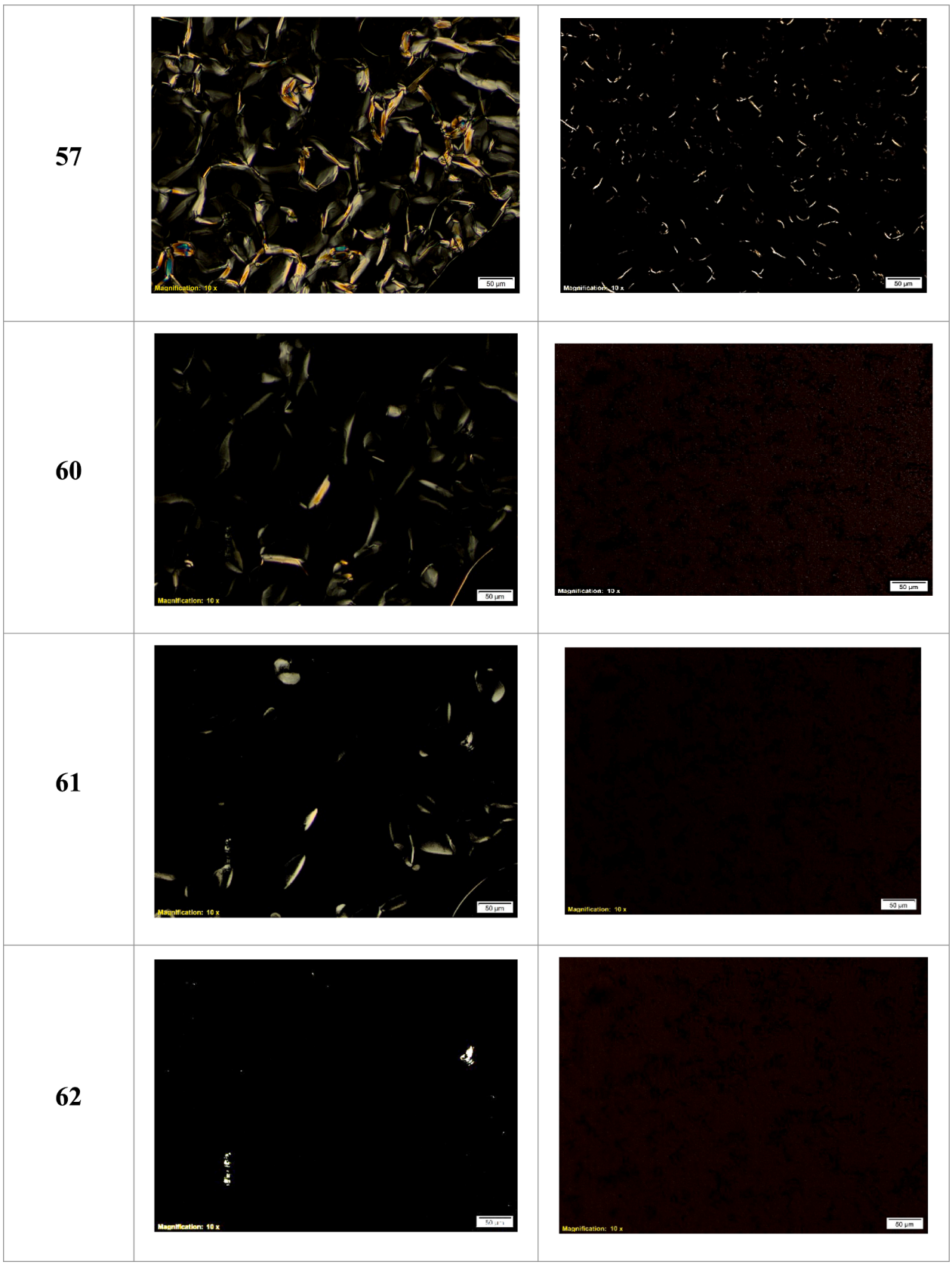

Fig. 5. (*continued*).

cooling time. However, BP sample shows a dampening of the temperature drop which makes it to reach the equilibrium temperature after ca. 1800 s of cooling time, a much longer time than that required for neat bitumen. This dampening effect is clearly noticed in the cooling rate-time profile of BP sample compared to neat bitumen. Thus, a first peak at ca. 80 s related to bitumen-rich phase is followed by a slow

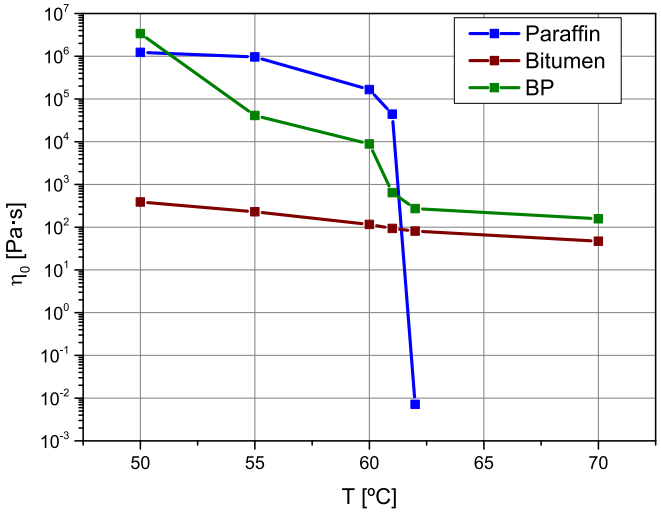

Fig. 6. Evolution of the zero-shear limiting viscosities (η_0) with temperature for bitumen, paraffin and bitumen/paraffin blend.

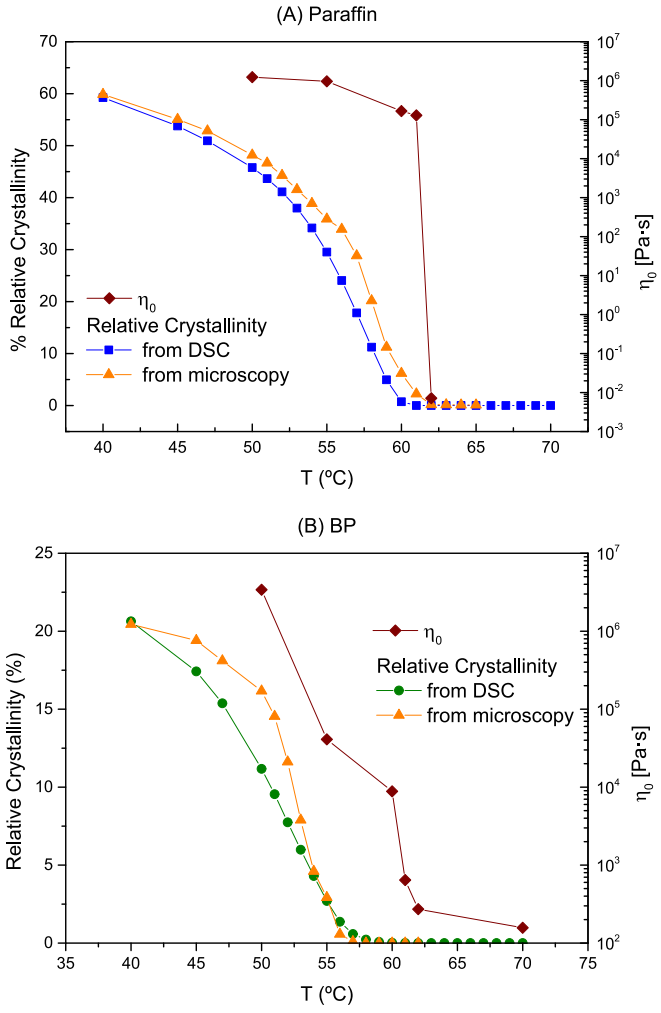

Fig. 7. Evolution with temperature of relative crystallinity obtained from DSC and for crossed polarised optical microscopy and zero-shear limiting viscosities for (A) paraffin and (B) bitumen/paraffin blend.

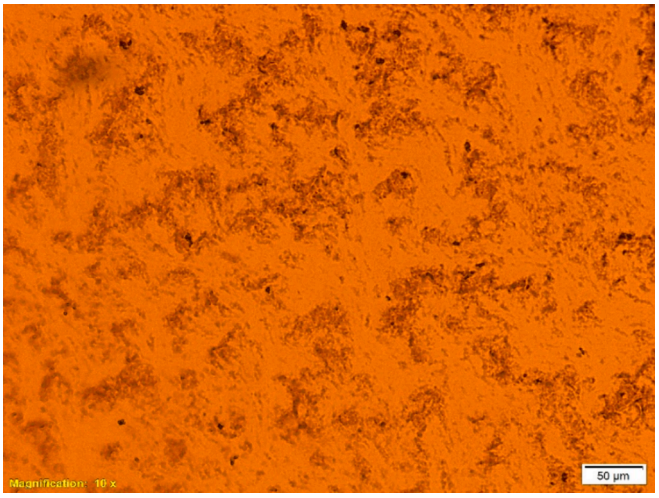

Fig. 8. Unpolarised optical microscopy image of bitumen/paraffin blends, at 70 °C.

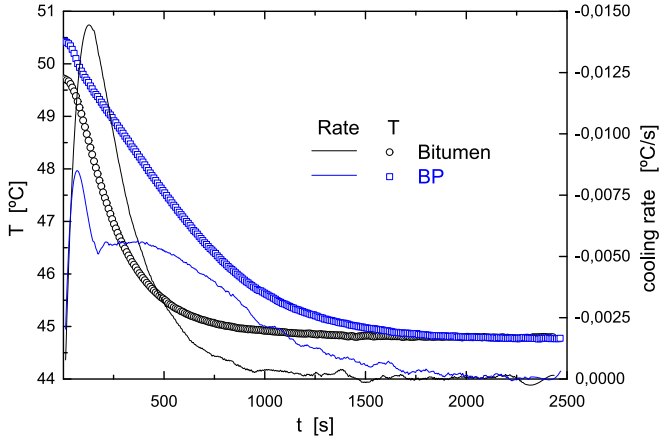

Fig. 9. Evolution of temperature and cooling rate for neat bitumen and bitumen/paraffin blend after a solar simulation test.

decrease consequence of the heat released in the course of the paraffin wax crystallization. Therefore, these results highlight the great potential of these formulations to be used in thermal energy storage and related applications with thermoregulation purposes.

4. Conclusions

According to the results, neat bitumen exhibits the well-known direct transition from the glassy to the Newtonian region with no relevant thermal events in the experimental window. In contrast, paraffin wax exhibits an intermediate mesophase region, between the glassy state and the isotropic liquid phase attributed to multiple solid-to-solid transitions between the so-called rotator phases. These are lamellar intermediate phases in which paraffin molecules may rotate or oscillate with a relatively large amplitude around their long axis, resulting in ordered structures but softer than the crystalline state.

The BP blend exhibits a multiphasic microstructure, wherein paraffin-rich and bitumen-rich phases form distinct domains at a microscale level, each retaining its own identity and displaying individual transitions. These phases influence on the thermorheological behaviour of the bulk differently as temperature increases.

The rheological results show a decrease of the complex shear modulus with temperature but also indicate a gel-like behaviour for both paraffin and paraffin/bitumen blend, which persists nearly until the end

of the phase change interval. This is due to the formation of a network of interconnected paraffin wax crystals, which gradually diminish as temperature rises. Remarkably, a weak gel structure persists even at low crystallinity levels, as only a few connections among structures are needed to form a spanning network. As the paraffin melts, the network of connected crystallites gradually disappears, resulting in a tenuous network that still retains a remarkable elastic character ($\delta < 45°$) and viscosity corresponding to the structured systems. As the temperature increases, more links are lost and the continuity of the network disappears, leading to a very marked decrease in the viscous and viscoelastic properties.

The presence of dispersed transitioning structures in BP lead to a relatively unusual flow behaviour, characterised by a viscosity overshoot in a narrow temperature range within melting. This effect can be explained by the formation of non-permanent physical networks, at specific strain rates, where interactions among structures lead to the formation of complex arrangements that restrict overall mobility.

Interestingly, at temperatures above the melting process, while paraffin completely transitions into the isotropic liquid state, BP develops a soft gel-like structure due to the persistence of its two-phase morphology, affecting its flow behaviour. Although the crystalline fraction then undergoes a similar evolution to that of paraffin wax, the morphology of the separated phases develops a new weak gel behaviour once melting is complete.

Finally, despite the partial compatibility between the bitumen-rich and paraffin-rich phases, the reduction in crystallinity is minimal. Thus, solar irradiation tests indicated the thermoregulation ability of BP sample compared to neat bitumen. Therefore, these results highlight the great potential of these bitumen-based formulations to be used for thermal energy storage, thermoregulation and similar applications. In general, bitumen/paraffin blend exhibits both enhanced thermal properties and rheological properties compared to neat paraffin wax, making it a suitable material to formulate form-stable products for solar thermal energy storage applications with thermoregulation purposes.

Declaration of competing interest

The authors declare that they have no known competing financial interests or personal relationships that could have appeared to influence the work reported in this paper.

Data availability

Data will be made available on request.

Acknowledgements

Grant TED2021-131284B-I00 funded by MCIN/AEI/ 10.13039/501100011033 (Spain) and grant PID2020-116905RB-I00 funded by MCIN/AEI/10.13039/501100011033 (Spain) and European Union "NextGenerationEU"/PRTR. Clara Delgado and Adrián Tenorio also acknowledge financial support from Junta de Andalucía (Spain) through post-doctoral Grants DC 01228 (co-funded by the European Union Fondo Social Europeo (FSE)) and POSTDOC_21_00644, respectively, Funding for open access charge: Universidad de Huelva / CBUA and the Cátedra Fundación CEPSA.

References

[1] R. Alvarez-Barajas, A.A. Cuadri, C. Delgado-Sánchez, F.J. Navarro, P. Partal, Polym. Test. 130 (2024) 108317, https://doi.org/10.1016/j.polymertesting.2023.108317.
[2] S. Rudyk, Relationships between SARA fractions of conventional oil, heavy oil, natural bitumen and residues, Fuel 216 (2018) 330–340, https://doi.org/10.1016/j.fuel.2017.12.001.
[3] G. Polacco, J. Stastna, D. Biondi, L. Zanzotto, Relation between polymer architecture and nonlinear viscoelastic behavior of modified asphalts, Curr. Opin. Colloid Interface Sci. 11 (2006) 230–245, https://doi.org/10.1016/j.cocis.2006.09.001.
[4] J. Kovinich, A. Kuhn, A. Wong, H. Ding, S.A.M. Hesp, Wax in Asphalt: A comprehensive literature review, Constr. Build. Mater. 342 (2022) 128011, https://doi.org/10.1016/j.conbuildmat.2022.128011.
[5] D.S. Nasir, C.A.J. Pantua, B. Zhou, B. Vital, J. Calautit, B. Hughes, Numerical analysis of an urban road pavement solar collector (U-RPSC) for heat island mitigation: impact on the urban environment, Renew Energy 164 (2021) 618–641, https://doi.org/10.1016/j.renene.2020.07.107.
[6] A.K. Hussein, F.L. Rashid, H. Togun, et al., A review of design parameters, advancement, challenges, and mathematical modeling of asphalt solar collectors, J. Therm. Anal. Calorim. (2023), https://doi.org/10.1007/s10973-023-12674-4.
[7] K. Wei, B. Ma, S.Y. Duan, Preparation and properties of bitumen-modified polyurethane solid–solid phase change materials, J. Mater. Civ. Eng. 31 (2019) 04019139, https://doi.org/10.1061/(ASCE)MT.1943-5533.0002795.
[8] M.R. Kakar, Z. Refaa, J. Worlitsfheck, A. Stamatiou, M.N. Partl, M. Bueno, Thermal and rheological characterization of bitumen modified with microencapsulated phase change materials, Constr. Build. Mater. 215 (2019) 171–179, https://doi.org/10.1016/j.conbuildmat.2019.04.171.
[9] M. Yang, X. Zhang, X. Zhou, B. Liu, X. Wang, X. Lin, Research and exploration of phase change materials on solar pavement and asphalt pavement: A review, J. Energy Storage 35 (2021) 102246, https://doi.org/10.1016/j.est.2021.102246.
[10] Y. Sheikh, M.O. Hamdan, S. Sakhi, A review on micro-encapsulated phase change materials (EPCM) used for thermal management and energy storage systems: Fundamentals, materials, synthesis and applications, J. Energy Storage 72 (2023) 108472, https://doi.org/10.1016/j.est.2023.108472.
[11] Y. Chen, H. Wang, Z. You, N. Hossiney, Application of phase change material in asphalt mixture – A review, Constr. Build. Mater. 263 (2020) 120219, https://doi.org/10.1016/j.conbuildmat.2020.120219.
[12] C. Gutiérrez-Blandón, A.A. Cuadri, A. Tenorio-Alfonso, P. Partal, F.J. Navarro, Rheological and phase behaviour of paraffin wax/bitumen blends with thermal storage characteristics, Constr. Build. Mater. 401 (2023) 132826, https://doi.org/10.1016/j.conbuildmat.2023.132826.
[13] Y. Lu, L. Liu, C. Wu, A. Liu, Y. Li1, R. Guo, J. Phys.: Conf. Ser. 1948 (2021) 012183.
[14] L. Najemi, I. Belyamani, M. Bouya, Effect of blending of medium-temperature phase change material on the bitumen storage heat, Heliyon 9 (11) (2023) e22040.
[15] H. Wang, Y. Wang, X. Li, M. Chen, Y. Wu, C. Sun, X. Wang, Antiaging property and mechanism of phase-change asphalt with PEG as an additive, Adv. Mater. Sci. Eng. 2020 (2020) 7598049, https://doi.org/10.1155/2020/7598049.
[16] D. Zhang, M. Chen, S. Wu, Q. Liu, J. Wan, Preparation of expanded graphite/polyethylene glycol composite phase change material for thermoregulation of asphalt binder, Constr. Build. Mater. 169 (2018) 513–521, https://doi.org/10.1016/j.conbuildmat.2018.02.167.
[17] M. Jia, A. Sha, W. Jiang, W. Wang, J. Li, J. Dai, Z. Lu, Laboratory evaluation of poly (ethylene glycol) for cooling of asphalt pavements, Constr Build. Mater. 273 (2021) 21774, https://doi.org/10.1016/j.conbuildmat.2020.121774.
[18] D.K. Bhamare, M.K. Rathod, J. Banerjee, Numerical model for evaluating thermal performance of residential building roof integrated with inclined phase change material (PCM) layer, J. Build. Eng. 28 (2020) 101018, https://doi.org/10.1016/j.jobe.2019.101018.
[19] C. Piselli, V.L. Castaldo, A.L. Pisello, How to enhance thermal energy storage effect of PCM in roofs with varying solar reflectance: Experimental and numerical assessment of a new roof system for passive cooling in different climate conditions, J. Sol. Energy 192 (2019) 106–119, https://doi.org/10.1016/j.solener.2018.06.047.
[20] F. Merusi, G. Polacco, S. Filippi, F. Giuliani, Structural transitions and physical networks in wax-modified bitumens, Road Mater. Pavement Des. 14 (2013) 289–309, https://doi.org/10.1080/14680629.2013.792292.
[21] S.A. Burrows, I. Korotkin, S.K. Smoukov, E. Boek, S. Karabasov, Benchmarking of molecular dynamics force fields for solid-liquid and solid-solid phase transitions in alkanes, J. Phys. Chem. B 125 (19) (2021) 5145–5159, https://doi.org/10.1021/acs.jpcb.0c07587.
[22] A. Abdi, M. Ignatowicz, S.N. Gunasekara, J.N.W. Chiu, V. Martin, Experimental investigation of thermo-physical properties of n-octadecane and n-eicosane, Int. J. Heat Mass Transf. 161 (2020) 120285, https://doi.org/10.1016/j.ijheatmasstransfer.2020.120285.
[23] M. Petersson, I. Gustafson, M. Stading, Comparison of microstructural and physical properties of two petroleum waxes, J. Mater. Sci. 43 (2008) 1869–1879, https://doi.org/10.1007/s10853-007-2417-9.
[24] E.M. Anghel, A. Georgiev, S. Petrescu, R. Popov, M. Constantinescu, Thermo-physical characterization of some paraffins used as phase change materials for thermal energy storage, J. Therm. Anal. Calorim. 117 (2014) 557–566, https://doi.org/10.1007/s10973-014-3775-6.
[25] H. Ding, H. Zhang, H. Zhang, D. Liu, Y. Qiu, A. Hussain, Separation of wax fraction in asphalt binder by an improved method and determination of its molecular structure, Fuel 322 (2022) 124081, https://doi.org/10.1016/j.fuel.2022.124081.
[26] E.S. Domalski, E.D. Hearing, Heat capacities and entropies of organic compounds in the condensed phase. Volume III, J. Phys. Chern. Ref. Data 25 (1996) 1–525, https://doi.org/10.1063/1.555985.
[27] A. Ribezzo, G. Falciani, L. Bergamasco, M. Fasano, E. Chiavazzo, An overview on the use of additives and preparation procedure in phase change materials for thermal energy storage with a focus on long term applications, J. Energy Storage 53 (2022) 105140, https://doi.org/10.1016/j.est.2022.105140.
[28] J. Wang, M.D. Calhoun, S.J. Severtson, Dynamic rheological study of paraffin wax and its organoclay nanocomposites, J. Appl. Polym. Sci. 108 (2008) 2564–2570, https://doi.org/10.1002/app.27768.

[29] D. Cholakova, K.T.S. Tcholakova, N. Denkov, Rheological properties of rotator and crystalline phases of alkanes, Colloids Surf. a: Physicochem. Eng. Asp. 634 (2022) 127926, https://doi.org/10.1016/j.colsurfa.2021.127926.
[30] P.K. Mukherjee, Renormalization-group analysis of the R(I)-R(V) rotator phase transition, J. Chem. Phys. 134 (22) (2011) 224502, https://doi.org/10.1063/1.3599051. PMID: 21682520.
[31] O.V. Laukkanen, H.H. Winter, H. Soenen, J. Seppälä, An empirical constitutive model for complex glass-forming liquids using bitumen as a model material, Rheol. Acta 57 (2018) 57–70, https://doi.org/10.1007/s00397-017-1056-6.
[32] M.J. Nowak, S.J. Severton, Dynamic mechanical spectroscopy of plastic crystalline states in n-alkane systems, J. Mater. Sci. 36 (2001) 4159–4166, https://doi.org/10.1023/A:1017908703339.
[33] H. Fang, W. Ye, Y. Ding, H. Henning Winter, Rheology of the critical transition state of an epoxy vitrimer, Macromolecules 53 (12) (2020) 4855–4862, https://doi.org/10.1021/acs.macromol.0c00843.
[34] P. Abivin, S.D. Taylor, D. Freed, Thermal behavior and viscoelasticity of heavy oils, Energy Fuel 26 (6) (2012) 3448–3461, https://doi.org/10.1021/ef300065h.
[35] M. Jasso, G. Polacco, L. Zanzotto, Shear viscosity overshoots in polymer modified asphalts, Materials 15 (2022) 7551, https://doi.org/10.3390/ma15217551.
[36] A.A. Cuadri, P. Partal, N. Ahmad, J. Grenfell, G. Airey, Chemically modified bitumens with enhanced rheology and adhesion properties to siliceous aggregates, Constr. Build. Mater. 93 (2015) 766–774, https://doi.org/10.1016/j.conbuildmat.2015.05.098.
[37] J.A. Lopes da Silva, J.A.P. Coutinho, Dynamic rheological analysis of the gelation behaviour of waxy crude oils, Rheol. Acta 43 (2004) 433–441, https://doi.org/10.1007/s00397-004-0367-6.
[38] H. Fatahi, J.P. Claverie, S. Poncet, Characterization by differential scanning calorimetry of thermal storage properties of organic PCMs with operating temperature of 150, ∘C J. Chem. Thermodynamics 186 (2023) 107136, https://doi.org/10.1016/j.jct.2023.107136.
[39] S. Acierno, E. Di Maio, S. Iannace, et al., Structure development during crystallization of polycaprolactone, Rheol. Acta. 45 (2006) 387–392, https://doi.org/10.1007/s00397-005-0054-2.